Stereoelectronic, Torsional, and Steric Effects on Rates of Enolization of Ketones

Shahrad M. Behnam,[†] Shahdad E. Behnam,[†] Kaori Ando,*[,‡] Nora S. Green,[†] and K. N. Houk*[,†]

Department of Chemistry and Biochemistry, University of California, Los Angeles, California 90095-1569, and College of Education, University of the Ryukyus, Nishihara-cho, Okinawa 903-0213, Japan

houk@chem.ucla.edu

Received June 14, 2000

The stereoselectivities of base-catalyzed enolizations of ketones have been studied by quantum mechanical methods. Transition structures of exo and endo deprotonation of camphor, norcamphor, and dehydronorcamphor have been located with two model bases. Stereoelectronic, torsional, and steric effects on activation energies were assessed. These calculations demonstrate the importance of torsional strain between partial bonds and vicinal bonds on the rates of deprotonation and on related reactions involving the formation of enolates or reactions of enols and enolates.

Introduction

The factors controlling the stereoselectivity of hydrogen exchange and enolate formation in the base-promoted reactions of cyclic ketones have been studied for several decades.[1−20] Experimental measurements of rates of exchange have been reported for the exo and endo hydrogens of bicyclic ketones such as camphor (**1**), norcamphor (**2**), and dehydronorcamphor (**3**). Table 1 illustrates the k_{exo}/k_{endo} deprotonation rate ratios for **1**, **2**, and **3** using a variety of techniques.[1−3] The k_{exo}/k_{endo} deprotonation rate ratios indicate a more rapid exchange of the exo hydrogen by deuterium compared to exchange of the endo hydrogen. NaOD-catalyzed exchange of **2** reveals a k_{exo}/k_{endo} rate ratio of 715, while the tritium counting technique[5] yields a smaller deprotonation rate of 81. Werstiuk et al. report a k_{exo}/k_{endo} ratio of 660 ± 66 for deuterioxide-catalyzed H → D exchange, whereas hydroxide-catalyzed D → H exchange in nondeuterated medium has a much smaller value of 72. Although the methods for measuring the exo and endo deprotonation rates of bicyclic ketones differ quantitatively, all demonstrate that the exo deprotonation is faster than the endo.[4−8] The $\Delta G^{\ddagger}$ for *exo* deprotonation is 1.5−4 kcal/mol lower than for *endo* deprotonation.

Table 1. Experimental exo/endo Ratios for Ketone Deprotonations

ketone	k_{exo}/k_{endo} mass spectroscopy	k_{exo}/k_{endo} tritium technique
1	21	4 ± 1
2	715[a]	81 ± 8
2	660 ± 66[b]	
2	72[c]	
3	120	19 ± 4
twistan-4-one	290	
4-methyl camphor	19	

[a] NaOD-catalyzed deprotonation−deuteration reaction at 25 °C in 2:1 dioxane/D_2O. [b] NaOD-catalyzed protium to deuterium exchange at 30 °C in 60% dioxane/D_2O. [c] Deuterium to protium exchange in a protic medium.

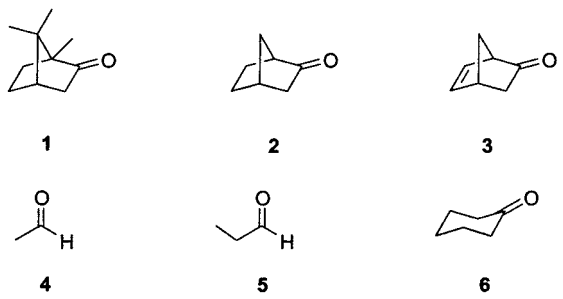

Orbital overlap or stereoelectronic effects,[9−13] van der Waals repulsion,[14−18] "nonequivalent orbital extenstion",[19]

[†] University of California, Los Angeles.
[‡] University of the Ryukyus.

(1) (a) Toullec, J. *Adv. Phys. Org. Chem.* **1982**, *18*, 1. (b) Tidwell, T. T. *J. Am. Chem. Soc.* **1970**, *92*, 1448.
(2) Lajunen, M.; Pilbacka, H. *Acta Chem. Scand.* **1976**, *30*, 391.
(3) Banerjee, S.; Werstiuk, N. H. *Can. J. Chem.* **1975**, *53*, 1099.
(4) Werstiuk, N. H.; Yeroushlami, S.; Guan-Lin, H. *Can. J. Chem.* **1992**, *70*, 974.
(5) (a) Lajunen, M., Ihantola, A.; Tallgren, J. *Acta Chem. Scand.* **1979**, *33*, 365. (b) Buncel, E.; Davey, J. P. *J. Chem. Soc., Perkin Trans. 2* **1990**, 169.
(6) Werstiuk, N. H.; Andrews, P. *Can. J. Chem.* **1978**, *56*, 2605.
(7) Stille, J. K.; Feld, W. A.; Freeburger, M. E. *J. Am. Chem. Soc.* **1972**, *94*, 8485.
(8) Brown, H. C.; Kawakami, J. H.; Ikegami, S. *J. Am. Chem. Soc.* **1970**, *92*, 6914.
(9) Corey, E. J.; Sneen, R. A. *J. Am. Chem. Soc.* **1956**, *78*, 6269.
(10) Abad, G. A.; Jindal, S. P.; Tidwell, T. T. *J. Am. Chem. Soc.* **1973**, *95*, 6326.
(11) Burgess, E. M.; Liotta, C. L. *J. Org. Chem.* **1981**, *46*, 1703.
(12) Wiberg, K. B. *Acc. Chem. Res.* **1999**, *922*, 2.
(13) Fraser, R. R.; Champagne, P. J. *J. Am. Chem. Soc.* **1978**, *100*, 657.
(14) Jindal, S. P.; Sohoni, S. S.; Tidwell, T. T. *Tetrahedron Lett.* **1971**, 779.
(15) Matthews, R. S.; Hyer, P. K.; Folkers, E. A. *J. Chem. Soc. D* **1970**, 38.
(16) Zimmerman, H. E. *Acc. Chem. Res.* **1987**, *20*, 263.
(17) Kayser, R. H.; Brault, M.; Pollack; R. M.; Bantia, S.; Sadoff, S. F. *J. Org. Chem.* **1983**, *48*, 4497.
(18) Pollack, R. M. *Tetrahedron* **1989**, *45*, 4913.
(19) (a) Inagaki, S.; Fujimoto, H.; Fukui, K. *J. Am. Chem. Soc.* **1976**, *98*, 4054. (b) Koga, N.; Ozawa, T.; Morokuma, K. *J. Phys. Org. Chem.* **1990**, *3*, 519. (c) Paquette, L. A.; Hsu, L.-Y.; Gallucci, J. C.; Korp, J. D.; Bernal, I.; Kravetz, T. M.; Hathaway, S. J. *J. Am. Chem. Soc.* **1984**, *106*, 5743.
(20) Rondan, N. G.; Paddon-Row: M. N.; Caramella, P.; Mareda, J.; Mueller, P. H.; Houk, K. N. *J. Am. Chem. Soc.* **1982**, *104*, 4974.

10.1021/jo000905v CCC: $19.00
Published on Web 11/28/2000

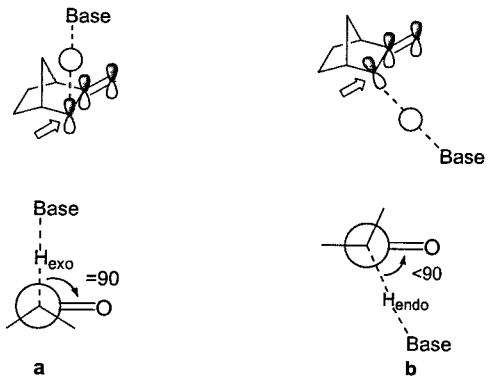

Figure 1. Potential stereoelectronic effect in norcamphor **(2)** deprotonation: **a** is the exo deprotonation of norcamphor by a base; **b** is the endo deprotonation of norcamphor by a base.

and torsional strain[20] have been cited as factors contributing to a faster rate of exo deprotonation. These factors are involved not only in base-promoted enolate formation but also in acid-catalyzed enol formation from ketones, protonation of enolates, alkylation of enolates, and decarboxylations of ketoacids. In this investigation, we examine the transition state structures for the deprotonation of **1**−**6** by several model bases using quantum mechanical methods. We have explored the general relationship between ketone geometry and the rate of deprotonation and have established which factors control the rates and stereoselectivities of deprotonations and related reactions.

Background

Stereoelectronic control in enolization was first proposed by Corey and Sneen[9] in 1956, and its importance was further emphasized by Abad et al.[10] and Burgess et al.[11] The stereoelectronic effect, referred to in this paper as the "CH-π overlap effect", is the stabilization resulting from the proper orbital overlap of the CH σ bond with the carbonyl π orbital as illustrated in Figure 1 for norcamphor. When the exo hydrogen is removed from the carbonyl compound by a base, the overlap of the developing p orbital with the π orbital contributes to the stabilization of the transition structure. However, the endo CH bond is situated such that the developing p orbital does not align as well with the carbonyl π orbital; the transition structure is stabilized less by developing enolate resonance. Wiberg has the emphasized electrostatic components of such resonance effects, but the geometrical constraints are the same.[12] In the original experiment of Corey and Sneen, acid-catalyzed enolization of 3β-acetoxycholestan-7-one to the Δ^6-en-7-ol using HBr as a catalyst in chloroform (Figure 2) showed that axial protonation occurs 1.2-fold faster than equatorial protonation. Correcting for an estimated steric effect, Corey and Sneen estimated a stereoelectronic effect favoring axial protonation by a factor of 12; this was postulated to be due to a CH-π overlap effect. Fraser and Champagne[13] found that base-catalyzed hydrogen exchange of twistan-4-one favors H_f exchange over H_s exchange by a ratio of 290:1 (Figure 3), and they cited such stereoelectronic factors as the main cause.

Steric effects, the van der Waals repulsion between nonbonded atoms, have been proposed to influence the k_{exo}/k_{endo} deprotonation rate ratios of many bicyclic ketones. Tidwell hypothesized that steric hindrance in base-catalyzed deuterium exchange of bicyclic ketones is important.[14] In norcamphor, the k_{exo}/k_{endo} ratio of base-catalyzed exchange is 715:1; the base is said to experience a steric effect when attacking the endo face.[14]

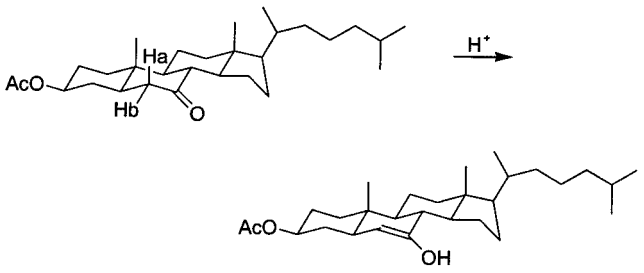

Figure 2. Acid-catalyzed enolization of 3β-acetoxycholestan-7-one to Δ^6-en-7-ol.

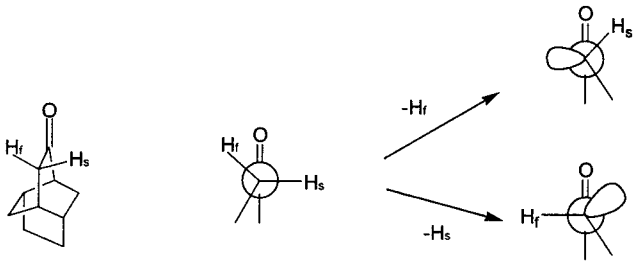

Figure 3. Base-catalyzed hydrogen exchange of twistan-4-one. Axial exchange is favored over equatorial exchange by a ratio of 290:1. H_f represents the faster deprotonating proton, and H_s represents the slow deprotonating proton.

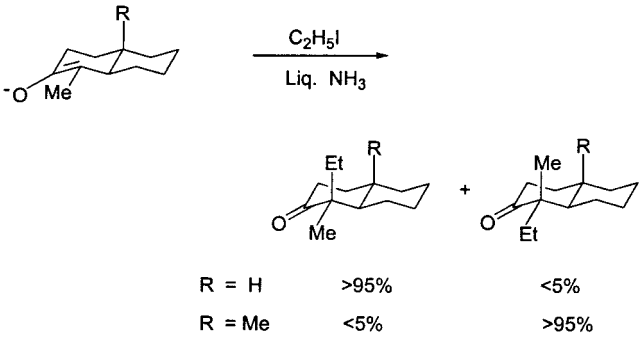

Figure 4. Steric factors on the alkylations of enolates.

The importance of steric effects is also illustrated by the results of Matthews et al.[15] on the alkylation of enolates. They found that the reaction between the enolate ion of 1-methyl-2-decalones and ethyl iodide gave different results depending on the presence or absence of a bridgehead substituent (Figure 4). With a methyl substituent, there is a severe steric hindrance to axial attack, leading to a favored equatorial attack by over 95%. However, with no substituents (R = H), the electrophile experiences no steric hindrance, and axial attack is favored by over 95%. Zimmerman has also illustrated that steric effects influence the face of ketone protonation.[16]

According to the model proposed by Corey and Sneen, the decarboxylation of 5-*tert*-butyl-1-methyl-2-oxocyclohexanecarboxylic acid (a β-ketoacid) should also be governed by stereoelectronic factors (Figure 5). However, Kayser et al.[17] demonstrated that the equatorial carboxyl is 15- to 20-fold more reactive in base than the axial

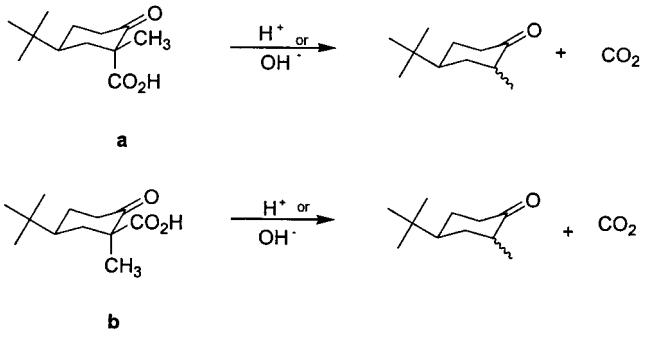

Figure 5. Decarboxylation of 5-*tert*-butyl-1-methyl-2-oxocyclohexanecarboxylic acid. The decarboxylation of **b**, the equatorial carboxyl group, is 15 to 20 times faster in base than that of **a**, the axial carboxyl group.

carboxyl group. This is an apparent contradiction to the CH-π overlap principal stated above, which would have predicted the axial carboxylate to decarboxylate more quickly.[18] It is conceivable that the anion of **b** is less stable than the anion of **a** as a result of a charge-dipole interaction, as the authors suggested.

Fukui and others[19] have proposed that norbornene and its derivatives undergo rapid exo attack as a result of a "nonequivalent orbital extension." There is believed to be mixing of the σ orbitals and π orbitals of the double bond, which leads to higher HOMO electron density on the exo face of the molecule. We have shown, however, that this is only a very small effect, since even alkenes which are highly pyramidalized show little sp mixing in the π bonds.[20]

Torsional strain involves the repulsion between vicinal bonds; the more nearly eclipsed, the larger the vicinal strain. Tidwell proposed that if torsional effects[21] were important, the eclipsing interaction between the C_4-CH_3 bond and the $C-H_{endo}$ of 4-methylcamphor should cause a more rapid exo deprotonation of 4-methylcamphor as compared to **1** (Table 1). The experiments indicate a slight decrease of k_{exo}/k_{endo} deprotonation rate ratios from 21 for **1** to 19 for 4-methylcamphor.[19] These authors concluded that torsional strain is not a critical contributor to deprotonation rates. However, it is now clear (see later) that CH, C−H torsional factors are as large as CMe, C−H, and so the nearly equal k_{exo}/k_{endo} ratios are consistent with the torsional explanation.

Computational Methods

Two models were employed to obtain the transition state geometries for the deprotonation of several bicyclic ketones. The first involves hydroxide as the base. The second involves hydroxide as a base solvated by one water molecule. The transition state structures for deprotonation by water-hydroxide were optimized with RHF/6-31G*. Single point energy calculations were then carried out with hybrid density functional theory using the 6-31G* basis set. The calculations involving unsolvated hydroxide were performed at the RHF/6-31+G* level. All calculations were performed using Gaussian 94.[22]

Results and Discussion

The overlap of the developing p orbital with the π orbital of the CO bond is essential for deprotonation. To assess the magnitude of this stereoelectronic effect, the proton transfer between acetaldehyde (**4**) and acetaldehyde enolate was studied to test quantitatively the relationship between dihedral angle and the rates of deprotonation (Figure 6). This system was studied earlier by Saunders[23] and Bernasconi.[24] The acetaldehyde enolate serves as the base and abstracts the proton from the acetaldehyde, forming a symmetrical transition structure (**8).** The energies required to distort **8** were calculated. The H−CCO dihedral angle on both acetaldehydes was fixed, and the remaining parameters were optimized. As the acetaldehyde transition structure is changed from ideal geometry to a geometry with both HCCO angles of 180°, the energy increases by 14.7 kcal/mol. As the HCCO angle decreases to 0°, the energy increases by 24.5 kcal/mol, since now there is loss of CH-π overlap and dipole−dipole repulsion involving the two C−O bonds. Since the dipole interaction is stabilizing for HCCC = 180° and destabilizing at 0°, we use the average of these energies to assess the magnitude of the CH−π overlap effect. It is 19.6 kcal/mol, or 9.8 kcal/mol per acetaldehyde molecule for maximum deviation of overlap from optimum in the transition state, to 0° or 180°, where overlap is zero.

Fraser and Champagne[13] postulated that the HCCO dihedral angle of 90° for twistan-4-one maximizes the orbital overlap between the π and σ orbitals, which allows for a faster rate of deprotonation. In the case of acetaldehyde, however, the ideal dihedral angle is 103° instead of 90°. This is presumably the result of repulsions between the base and the developing enolate oxygen. Such a dihedral angle also exists for other complex ketone systems, and distortions away from such an angle will also produce an energetically unfavorable molecule with lower deprotonation rates.

We have shown earlier how torsional effects involving single bonds and partially formed bonds in transition states influence the rates and stereoselectivities of a variety of reactions.[25] The deprotonation of propanal (**5**) was studied to test the magnitude of torsional effects involving vicinal bonds in these reactions (Figure 7). The staggered (**5a)** and the eclipsed (**5b)** transition structures of propanal deprotonation by hydroxide anion were studied. In the eclipsed conformation, the HCCH dihedral angle was fixed to 0.0°. The staggered transition state

(21) (a) Jindal, S. P.; Tidwell, T. T. *Tetrahedron Lett.* **1971**, 738. (b) Schleyer, P. V. R. *J. Am. Chem. Soc.* **1967**, *89*, 701.

(22) Frisch, M. J.; Trucks, G. W.; Schlegel, H. B.; Gill, P. M. W.; Johnson, B. G.; Robb, M. A.; Cheeseman, J. R.; Keith, T.; Petersson, G. A.; Montgomery, J. A.; Raghavachari, K.; Al-Laham, M. A.; Zakrzewski, V. G.; Ortiz, J. V.; Foresman, J. B.; Cioslowski, J.; Stefanov, B. B.; Nanayakkara, A.; Challacombe, M.; Peng, C. Y.; Ayala, P. Y.; Chen, W.; Wong, M. W.; Andres, J. L.; Replogle, E. S.; Gomperts, R.; Martin, R. L.; Fox, D. J.; Binkley, J. S.; Defrees, D. J.; Baker, J.; Stewart, J. P.; Head-Gordon, M.; Gonzalez, C.; Pople, J. A. *Gaussian 94*, Revision C.2; Gaussian Inc.: Pittsburgh, 1995.

(23) Saunders: W. H. *J. Am. Chem. Soc.* **1994**, *116*, 5400.

(24) (a) Bernasconi, C. F.; Wenzel, P. J. *J. Am. Chem. Soc.* **1994**, *116*, 5405. (b) Bernasconi, C. F.; Wenzel, P. J. *J. Am. Chem. Soc.* **1996**, *118*, 10494.

(25) (a) Wu, Y.-D.; Houk, K. N. *J. Am. Chem. Soc.* **1987**, *109*, 908. (b) Wu, Y.-D.; Houk, K. N.; Florez, J.; Trost, B. M. *J. Org. Chem.* **1991**, *56*, 3656. (c) Ando, K.; Houk, K. N.; Busch, J.; Menasse, A.; Suquin, U. *J. Org. Chem.* **1998**, *63*, 1761. (d) Ando, K.; Condroski, K. R.; Houk, K. N.; Wu, Y.−D.; Ly, S. K. Overman, L. E. *J. Org. Chem.* **1998**, *63*, 3196. (e) Eksterowicz, J. E.; Houk, K. N. *Chem. Rev.* **1993**, *93*, 2439. (f) Wu, Y.-D.; Tucker, J. A.; Houk, K. N. *J. Am. Chem. Soc.* **1991**, *113*, 5018. (g) Wu, Y.-D.; Houk, K. N. *J. Am. Chem. Soc.* **1993**, *115*, 10992. (h) Wu, Y.-D.; Houk, K. N.; Paddon-Row: M. N. *Angew. Chem., Int. Ed. Engl.* **1992**, *31*, 1019. (i) Lucero, M. J.; Houk, K. N. *J. Am. Chem. Soc.* **1997**, *119*, 826. (j) Martinelli, M. J.; Peterson, B. C.; Khau, V. V.; Hutchinson, D. R.; Leanna, M. R.; Audia, J. E.; Droste, J. J.; Wu, Y.-D.; Houk, K. N. *J. Org. Chem.* **1994**, *59*, 2204. (k) Ando, K.; Li, Y.; Green, N. S.; Houk, K. N. *J. Am. Chem. Soc.* **1999**, *121*, 5334.

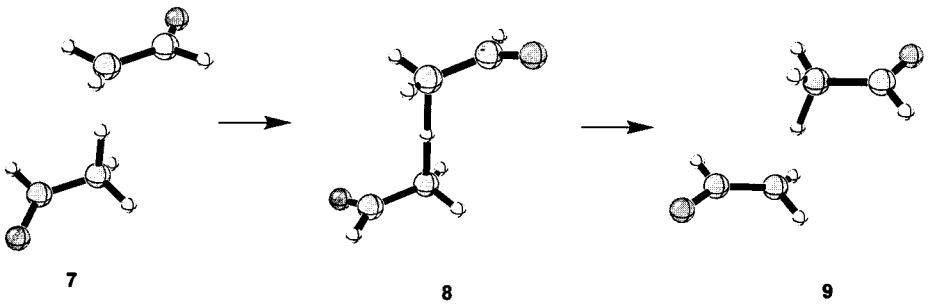

HCCO dihedral angle and relative energy of proton transfer transition state.

HCCO Dihedral Angle	Energy of **8** (kcal/mol)
0°	24.5
30°	16.6
60°	6.5
90°	0.6
103°	0.0
120°	1.1
145°	6.0
160°	10.2
180°	14.7

Figure 6. Acetaldehyde−acetaldehyde enolate deprotonation reaction.

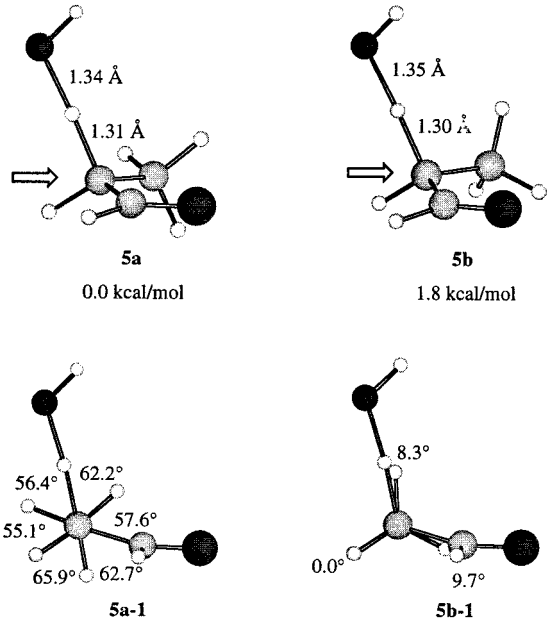

Figure 7. Transition structures for the deprotonation reaction of propanal, **5**, with hydroxide anion (RHF/6-31+G*). **5a** is the staggered transition structure and **5b** is the eclipsed transition structure. $\Delta E_{\text{eclipsed-staggered}} = +1.8$ kcal/mol. **5a**-1 and **5b**-1 are Newman projections from the direction of the arrow.

5a is 1.8 kcal/mol more favorable than **5b**. The HCCO dihedral angles of **5a** and **5b** are 104.8° and 104.4°, respectively. Since **5a** is not significantly more stabilized by orbital overlap than **5b**, the higher rate of deprotonation in the staggered conformer can only be attributed to the more favorable torsional effects for this case.

For the deprotonation of camphor (**1**) by a hydroxide anion, the exo transition state (**1b**) is favored over the endo transition state (**1a**) by 1.0 kcal/mol (Figure 8). This energy difference corresponds to a product ratio of 5.4:1 at 298 K, which is of the same order of magnitude as the experimental results (Table 1). With regards to steric effects, there are repulsive interactions during the endo deprotonation between the hydrogen of C_5 and the oxygen of the incoming base, as well as the proton being removed. The corresponding distances are 2.46 and 2.21

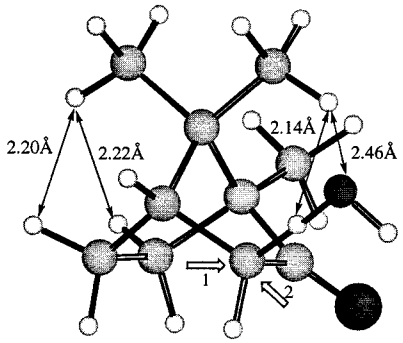

Å, respectively. Similarly, in the exo deprotonation, there are repulsive interactions between the hydrogen of C_9 and these atoms. The distances are 2.46 and 2.14 Å, respectively. Thus, the steric environments for **1a** and **1b** are nearly equivalent and do not favor the deprotonation rate of one over the other. With respect to stereoelectronic factors, the Newman projections **1a**-1 and **1b**-1, from the direction indicated by arrow 1, show that the HCCO dihedral angles are 71.0° and 69.4° for **1a** and **1b**, respectively. Thus, **1a** and **1b** have about the same amount of the conjugative stabilization by the carbonyl π orbital, and this cannot be the cause for the higher deprotonation rate of **1a.** Torsional strain, however, can explain the energy difference between **1a** and **1b**. As shown in the Newman projections, **1a**-2 and **1b**-2, from the direction indicated by arrow 2, endo deprotonation occurs with a rather eclipsed arrangement, while **1b** exhibits a more staggered arrangement. Thus, such torsional differences can influence deprotonation rates and account qualitatively for the 4−21 *exo*/*endo* rate ratios.

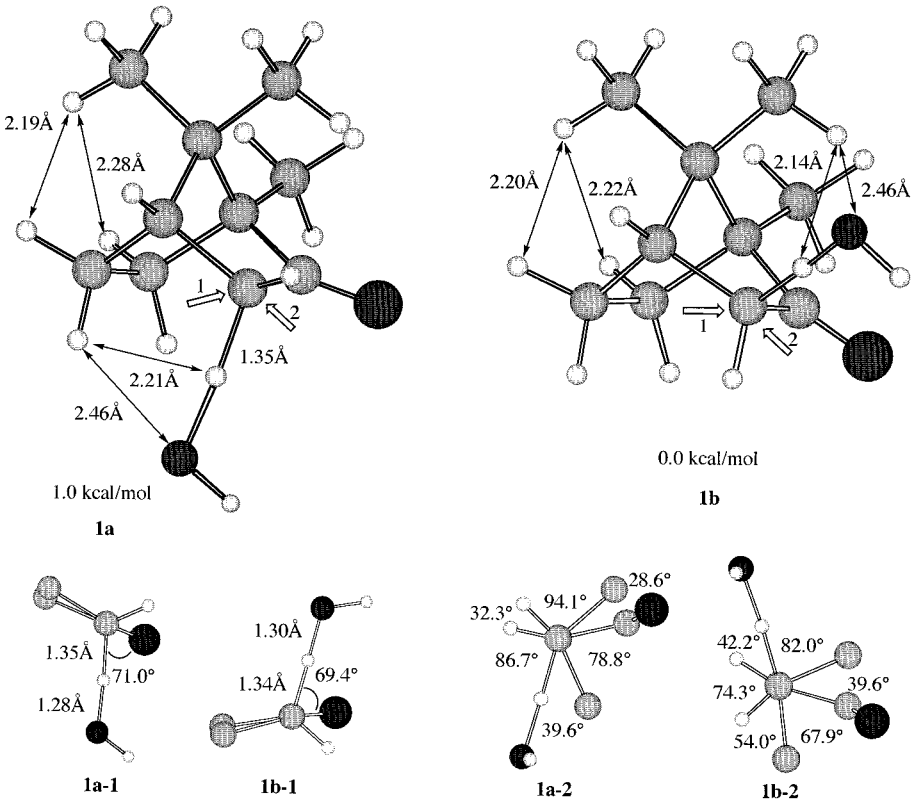

Figure 8. Transition structures for the deprotonation reaction of camphor, **1**, with hydroxide anion (RHF/6-31+G*). **1a** is the endo transition structure, and **1b** is the exo transition structure. $\Delta E_{endo-exo} = +1.0$ kcal/mol. **1a-1** and **1b-1** are Newman projections from the direction of the arrow 1. **1a-2** and **1b-2** are Newman projections from the direction of the arrow 2.

For the deprotonation of norcamphor (**2**) by water hydroxide complex, the exo transition structure (**2b**) is 3.1 kcal/mol more favorable than the endo transition structure (**2a**) (Figure 9A). This energy difference equals a product ratio of 191:1 at 298 K. Again, this is of the same order of magnitude as the experimental results. There are repulsive interactions during the endo deprotonation involving the hydrogen of C_5, the hydrogen being removed, and the oxygen of the incoming base. The nonbonding distances are shown in Figure 9A. These van der Waals repulsions hinder endo deprotonation and, as a result increase k_{exo}/k_{endo} ratio. The stereoelectronic factors demonstrated by Newman projections **2a**-1 and **2b**-1, indicated by arrow 1, show that the endo and exo HCCO dihedral angles are 70.5° and 74.1°, respectively. Since the HCCO dihedral angle of **2b** is closer to the optimal angle of 103°, it achieves a greater stabilization by orbital overlap, which contributes to a faster deprotonation rate. Additionally, torsional factors demonstrated by Newman projections **2a-**2 and **2b-**2, indicated by arrow 2, show that **2b** has a nearly staggered transition state conformation with respect to C2−C3, while **2a** has an almost eclipsed conformation.

Using the hydroxide model, the exo transition state **2d** is favored over the endo transition state (**2c**) by 2.7 kcal/mol (Figure 9B). In the endo transition structure **2c**, there is a repulsive interaction between the C_5 hydrogen, the hydrogen being removed, and the hydroxide oxygen. These distances are 2.30 Å and 2.52 Å, respectively. Newman projections, **2c**-1 and **2d**-1, from the direction of arrow 1, show that the HCCO dihedral angles are 71.8° and 81.1° for **2c** and **2d**, respectively. **2d** enjoys greater stabilization by CH-π orbital overlap. Also the Newman projections from the direction indicated by arrow 2, **2c**-2 and **2d**-2, show that **2c** has a rather eclipsed arrangement, while **2d** has a nearly perfectly staggered arrangement of all vicinal bonds. Thus, steric, electronic and torsional factors all favor the exo transition structures **2b** and **2d**. The 3.1 kcal/mol energy difference between **2a** and **2b** (water hydroxide complex model) and the 2.7 kcal/mol energy difference between **2c** and **2d** (hydroxide anion model) can be understood as resulting from these factors.

For the deprotonation of dehydronorcamphor **3** in the water hydroxide model, the exo transition structure **3b** is 3.8 kcal/mol more favorable than the endo transition structure **3a** (Figure 10A). The Newman projections **3a**-1 and **3b**-1, indicated by arrow 1, show that the HCCO dihedral angle is 71.5° for **3a** and 74.1° for **3b**. Thus, the exo transition structure is more stabilized by the greater overlap between the p orbital of the α carbon and the carbonyl π orbital, but the magnitude of this effect according to the calculations in Figure 6 is only about 0.2 kcal/mol. Additionally, Newman projections **3a**-2 and **3b**-2, indicated by arrow 2, illustrate that **3b** has a staggered geometry while **3a** has a more eclipsed arrangement. The higher rate of exo reactivity can be attributed to both the more staggered conformation of **3b** as well as the greater stabilization of **3b** by the stereoelectronic effect. The two kinds of transition states for deprotonation of **3** with hydroxide anion were also calculated (Figure 10B). The exo transition structure **3d** has a lower energy than the endo transition structure **3c** by 3.2 kcal/mol even though there is a small steric repulsion between the proton being abstracted and the bridgehead proton (2.37 Å) in **3d**. As shown in the

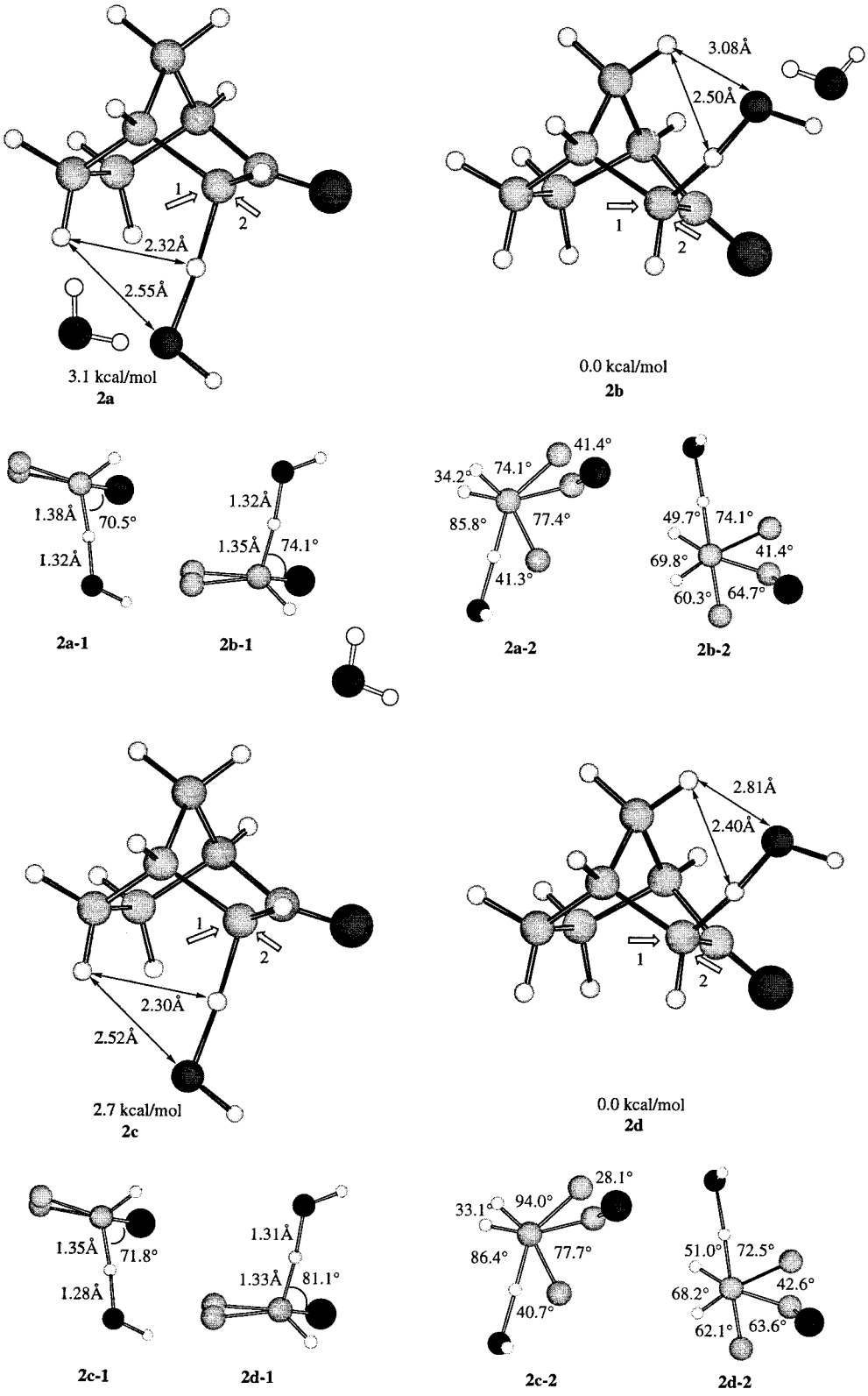

Figure 9. A: Transition structures for the deprotonation reaction of norcamphor, **2**, with water−hydroxide complex (Becke3LYP/6-31G*//RHF/6-31G*). **2a** is the endo transition structure, and **2b** is the exo transition structure. $\Delta E_{endo-exo} = +3.1$ kcal/mol. **2a-1** and **2b-1** are Newman projections from the direction of the arrow 1. **2a-2** and **2b-2** are Newman projections from the direction of the arrow 2. **B**: Transition structures for the deprotonation reaction of norcamphor, **2**, with hydroxide anion (RHF/6-31+G*). **2c** is the endo transition structure, and **2d** is the exo transition structure. $\Delta E_{endo-exo} = +2.7$ kcal/mol. **2c-1** and **2d-1** are Newman projections from the direction of the arrow 1. **2c-2** and **2d-2** are Newman projections from the direction of the arrow 2.

Newman projections, **3c**-1 and **3d**-1, from the direction of arrow 1, the HCCO dihedral angles are 69.5° and 78.0° for **3c** and **3d**, respectively. Again, **3d** is stabilized more efficiently by CH-π overlap than **3c**, and the nearly 10° difference might lead to ~0.9 kcal/mol difference in energy. The Newman projections from the direction of

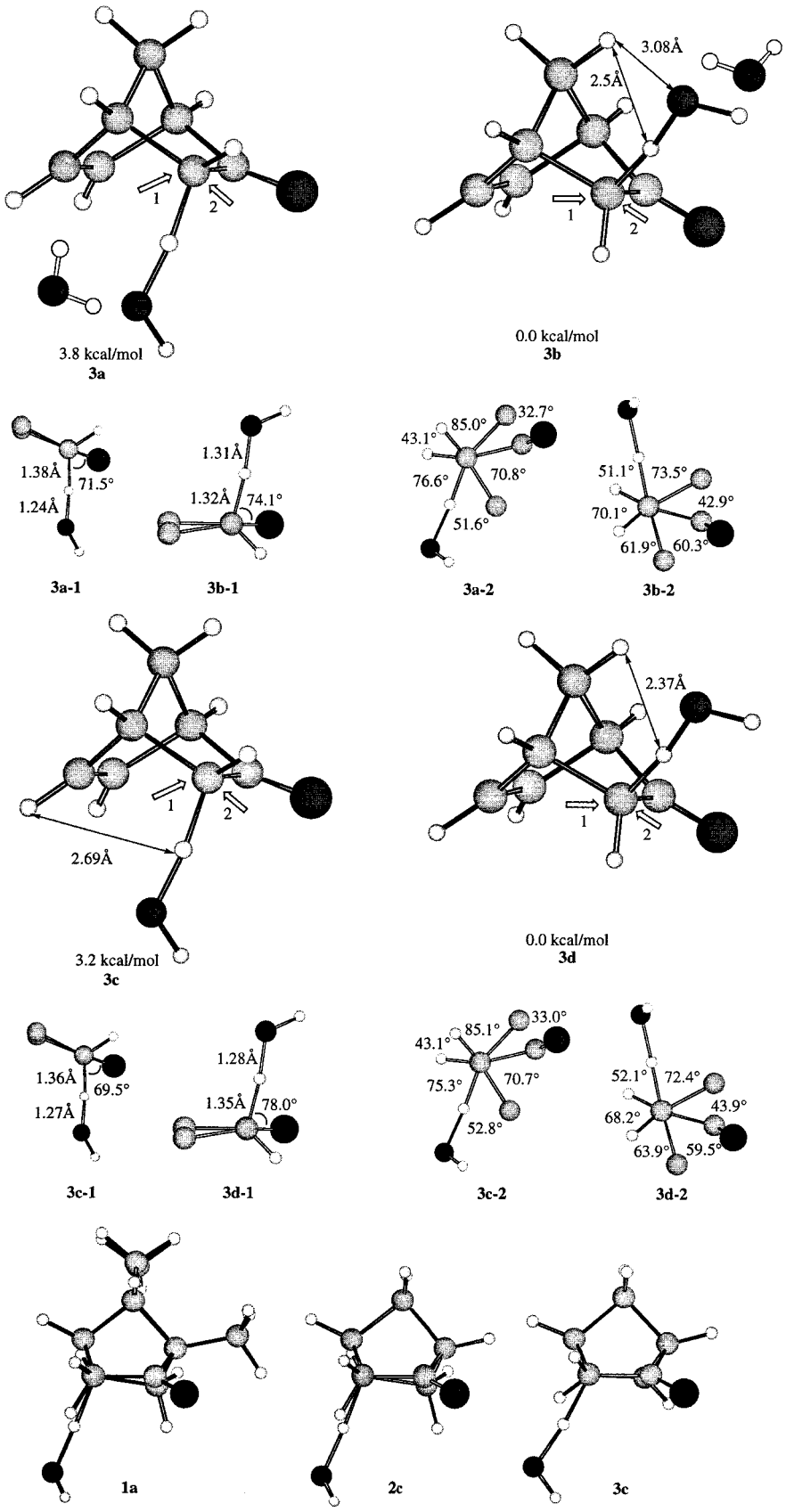

Figure 10. A: Transition structures for the deprotonation reaction of dehydronorcamphor, **3**, with water−hydroxide complex (Becke3LYP/6-31G*). **3a** is the endo transition structure, while **3b** is the exo transition structure. $\Delta E_{\text{endo-exo}} = +3.8$ kcal/mol. **3a-1** and **3b-1** are Newman projections from the direction of the arrow 1. **3a-2** and **3b-2** are Newman projections from the direction of the arrow 2. **1a**, **2c**, and **3c** show that the hydroxide ion is moved away from the double bond in **3c** relative to **1a** and **2c. B**: Transition structures for the deprotonation reaction of dehydronorcamphor, **3**, with hydroxide ion (RHF/6-31+G*). **3c** is the endo transition structure, and **3b** is the exo transition structure. $\Delta E_{\text{endo-exo}} = +3.2$ kcal/mol. **3c-1** and **3d-1** are Newman projections from the direction of the arrow 1. **3c-2** and **3d-2** are Newman projections from the direction of the arrow 2.

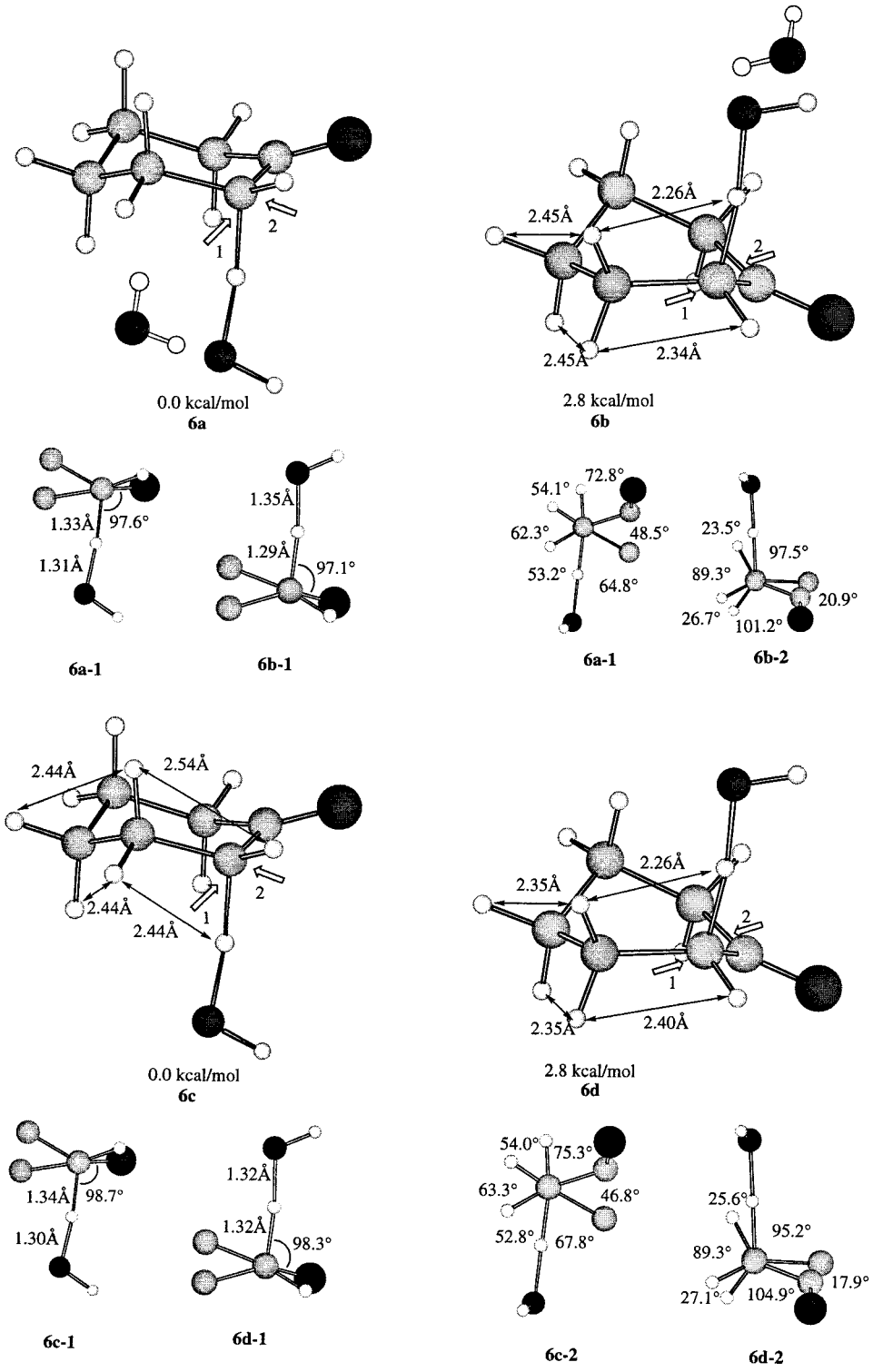

Figure 11. A: Transition structures for the deprotonation reaction of cyclohexanone, **6**, with water−hydroxide complex (RHF/6-31G*). **6a** is the axial transition structure and **6b** is the equitorial transition structure. $\Delta E_{eq-ax} = +2.8$ kcal/mol. **6a-1** and **6b-1** are Newman projections from the direction of the arrow 1. **6a-2** and **6b-2** are Newman projections from the direction of the arrow 2. **B**: Transition structures for the deprotonation reaction of cyclohexanone, **6**, with hydroxide ion (RHF/6-31+G*). **6c** is the axial transition structure and **6d** is the equatorial transition structure. $\Delta E_{eq-ax} = +2.8$ kcal/mol. **6c-1** and **6d-1** are Newman projections from the direction of the arrow 1. **6c-2** and **6d-2** are Newman projections from the direction of the arrow 2.

arrow 2, **3c**-2 and **3d**-2, show that **3c** has a more eclipsed arrangement than **3d**. Judging from the energy difference between **5a** and **5b**, this could provide *less than* a 1.0 kcal/mol preference for exo deprotonation. These two factors are not enough to explain the 3.2 kcal/mol difference in energy. Since **3** has an extra double bond on the endo face, electrostatic repulsions between the hydroxide and the π electrons of the double bond are plausible. In fact, **1a**, **2c**, and **3c** at a different angle show that hydroxide is moved away from the double bond in

3c relative to **1a** and **2c**. Thus, π overlap, torsional strain, and electrostatic repulsion all favor the exo transition states **3b** and **3d**, while steric repulsions disfavor **3d**.

Even though norcamphor and dehydronorcamphor exhibit similar k_{exo}/k_{endo} ratios, the enolate of norcamphor forms much more readily experimentally.[1−3] The calculated activation energy for exo deprotonation of norcamphor is 1.5 kcal/mol less than that of dehydronorcamphor from RHF/6-31+G* calculation. It is possible that the developing homoantiaromatic interaction between the face-to-face double bonds in the dehydronorcamphor enolate destabilizes this transition state. Destabilization of related anions by homoantiaromatic interactions has been postulated.[26]

The transition states for deprotonation of cyclohexanone (**6**) were calculated in order to compare with the structurally rigid ketones. In both the water hydroxide complex model and the hydroxide anion model, the cyclohexanone transition structures **6a** and **6c**, corresponding to the abstraction of an axial proton, are favored over **6b** and **6d** for the abstraction of an equatorial proton, by 2.8 kcal/mol (Figure 11A and B). The attempt to remove the equatorial hydrogen from the chair conformation effected a reorganization to the half-chair where the hydrogen becomes pseudoaxial. The Newman projections for **6a**−**d**-1 show that they all fully enjoy conjugative stabilization by overlap of the breaking CH bond with the carbonyl group π orbital. There is no relationship between reactant CH−π overlap and that found in the transition state. To make the reaction feasible and to maintain this conjugative stabilization, **6b** and **6d** flip into half-chair structures, resulting in unfavorable torsional and steric effects. The Newman projections from the direction of arrow 2 show that **6b** and **6d** occur with a rather eclipsed arrangement, while **6a** and **6c** exhibit a nearly perfectly staggered arrangement of all vicinal bonds. Thus, steric and torsional effects favor transition structures **6a** and **6c** for axial deprotonation by 2.8 kcal/mol.

Conclusion

Transition structures for deprotonation of a variety of carbonyl compounds have been located. The importance of stereoelectronic, torsional, and steric factors have been determined. In the cases studied, differing conjugative stabilization by CH−π orbital overlap does not directly influence stereoselectivity, because the breaking CH bond is nearly always in the optimum geometry in the transition state. Although steric effects are present in every case studied, they are not large enough to cause the several kcal/mol energy difference seen between the transition structures. Steric effects only dominate in exceptionally crowded cases. However, torsional strain involving vicinal bonds contributes significantly to the stereoselectivity in all of the cases studied. This factor is consistent with torsional effects identified for a variety of reactions, some closely related to ketone deprotonations.[25]

Acknowledgment. We are grateful to the National Institute of General Medical Sciences, National Institutes of Health for financial support of this research.

JO000905V

(26) (a) Breslow, R.; Pagni, R.; Washburn, W. *Tetrahedron Lett.* **1970**, 547. (b) Davis, D. D.; Bigelow, W. B. *Tetrahedron Lett.* **1973**, 149. (c) Houk, K. N.; Gandour, R. W.; Strozier, R. W.; Rondan, N. G.; Paquette, L. A. *J. Am. Chem. Soc.* **1979**, *101*, 6797. (d) Wilcox, C. F., Jr.; Blain, D. A.; Clardy, J.; Duyne, G. V.; Gleiter, R.; Eckert-Maksic, M. *J. Am. Chem. Soc.* **1986**, *108*, 7693. (e) Williams, R. V.; Kurtz, H. A. *Adv. Phys. Org. Chem.* **1994**, *29*, 273.